J Korean Med Sci 2007; 22: 633-40
ISSN 1011-8934

Decreased Left Ventricular Torsion and Untwisting in Children with Dilated Cardiomyopathy

The purpose of this study was to analyze left ventricular (LV) torsion and untwisting, and to evaluate the correlation between torsion and other components of LV contraction in children with dilated cardiomyopathy (DCM). Segmental and global rotation, rotational rate (V*rot*) were measured at three levels of LV using the two-dimensional (2D) speckle tracking imaging (STI) method in 10 DCM patients (range 0.6-15 yr, median 6.5 yr, 3 females) and 17 age- and sex-matched normal controls. Global torsion was decreased in DCM (peak global torsion; 10.9±4.6° vs. 0.3±2.1°, p<0.001). Loss of LV torsion occurred mainly by the diminution of counterclockwise apical rotation and was augmented by somewhat less reduction in clockwise basal rotation. In DCM, the normal counterclockwise apical rotation was not observed, and the apical rotation about the central axis was clockwise or slightly counterclockwise (peak apical rotation; 5.9±4.1° vs. -0.9±3.1°, p<0.001). Systolic counterclockwise V*rot* and early diastolic clockwise V*rot* at the apical level were decreased or abolished. In DCM, decreased systolic torsion and loss of early diastolic recoil contribute to LV systolic and diastolic dysfunction. The STI method may facilitate the serial evaluation of the LV torsional behavior in clinical settings and give new biomechanical concepts for better management of patients with DCM.

Key Words : *Torsion; Rotation; Left Ventricle; Dilated Cardiomyopathy*

Seon Mi Jin*, Chung Il Noh, Eun Jung Bae, Jung Yun Choi, Yong Soo Yun

Department of Pediatrics, Seoul National University Children's Hospital, Seoul National University College of Medicine, Seoul; Department of Pediatrics*, Eulji Medical Center, Eulji University, Seoul, Korea

Received : 26 October 2006
Accepted : 11 January 2007

Address for correspondence
Chung Il Noh, M.D.
Department of Pediatrics, Seoul National University Children's Hospital, 28 Yeongeon-dong, Jongro-gu, Seoul 110-744, Korea
Tel : +82.2-2072-3632, Fax : +82.2-743-3455
E-mail : ksydhnoh@yahoo.co.kr

INTRODUCTION

Rotation of the left ventricular (LV) apex relative to the base is related to the myocardial contractility and multilayer fiber orientations, and is a key parameter of cardiac performance (1-3). LV torsion and untwisting overall showed age-related increases, and when normalized by LV length, they showed higher values in infancy and middle age (4). Recent studies reported impaired rotation and torsion in tachycardia-induced dilated cardiomyopathy (DCM) animals and DCM patients (5, 6). Although this wringing motion can give novel insights into LV function, it is difficult to measure practically. A noninvasive and simple method for measurements of LV torsion is warranted to facilitate widespread and serial evaluation of the torsional behavior in clinical settings and to reveal the relationships between torsional alterations and clinical outcomes in various pathologic states. The two-dimensional (2D) speckle tracking imaging (STI) method, a novel ultrasound method for quantification of regional deformation, allows visualization and quantification of true 2D heart motion independent of borders, Doppler or its beam angles. It also enabled quantification of rotation and rotational rate (V*rot*) in an objective manner (7). In the present study, we sought to analyze LV torsion and untwisting using the new STI method, and evaluated the correlation between torsion and other components of LV contraction in children with DCM.

MATERIALS AND METHODS

Study populations

Between January and December 2005, 10 consecutive patients with DCM (range 0.5-15 yr, median age 6.5 yr, mean age 5.9±4.6 yr, 3 females) and 17 age- and sex-matched normal controls (range 0.5-14 yr, median age 5 yr, mean age 6.0 ±4.2 yr, 5 females) were enrolled into this study. Normal controls were obtained from children referred for electrocardiography or echocardiography, and who had no evidence of heart disease by physical examination, electrocardiography or echocardiography. There were no significant differences in clinical profiles between the DCM group and normal controls (p>0.05) (Table 1). The protocol was approved by the Ethics Committee of Seoul National University (Seoul, Korea), and informed consent was obtained before the study from all patients and/or their parents.

Table 1. Clinical profiles, conventional 2-dimensional echocardiographic, tissue Doppler imaging and 2-dimensional speckle tracking imaging data of study subjects

	Normal controls	DCM patients	*p* value
Number	17	10	
Age (yr)	6.0±4.2	5.9±4.6	0.955
% of female	30	35	0.847
Body weight (kg)	22.9±15.8	22.4±17.9	0.948
BSA (m^2)	0.82±0.38	0.79±0.41	0.848
2D echocardiographic data			
EDVI (mL/m^2)	51.3±9.8	90±24.5	0.001
ESVI (mL/m^2)	21.9±5.3	65.2±30.6	0.003
Ejection fraction (%)	58.6±5.9	26.5±13.3	<0.001
Tissue Doppler imaging data			
Long axis function			
Septal S' (cm/sec)	7.4±1.0	4.6±2	0.005
Septal E' (cm/sec)	11.7±2.5	7±2.1	0.003
Lateral S' (cm/sec)	7.1±1.8	5.3±2.5	0.01
Lateral E' (cm/sec)	13.5±2	9.1±4	0.004
2D STI data			
Short axis function			
Radial motion at MV level			
Sr (%)	42.2±12.7	15.7±7.6	<0.001
SRrs (1/sec)	2.4±0.6	1.1±0.4	<0.001
SRre (1/sec)	-2.5±1.1	-1.6±0.7	0.01
Circumferential motion at MV level			
Sc (%)	-15.7±3.8	-9.5±3.6	<0.001
SRcs (1/sec)	-1.5±0.5	-1.0±0.4	0.05
SRce (1/sec)	1.9±0.4	1.1±0.5	0.003

Data shown as means±SD.
DCM, dilated cardiamyopathy; BSA, body surface area; EDVI (mL/m^2), end diastolic volume index; ESVI (mL/m^2), end systolic volume index; S', peak systolic velocity of myocardial tissue Doppler at LV base; E', peak early diastolic velocity of myocardial tissue Doppler at LV base; 2D STI, 2 dimensional speckle tracking imaging; MV, mitral valve; Sr, peak radial strain; SRrs, peak systolic radial strain rate; SRre, peak early diastolic radial strain rate; Sc, peak circumferential strain; SRcs, peak systolic circumferential strain rate; SRce, peak early diastolic circumferential strain rate.

Conventional and tissue Doppler echocardiography

The main examinations were performed with Vivid 7 scanner (GE Vingmed Ultrasound, Horten, Norway) equipped with a phased-array transducer. Echocardiograms were evaluated by two physicians. LV end-systolic volume index (ESVI), end-diastolic volume index (EDVI), and ejection fraction (EF) were calculated as previously described (8, 9). To assess LV longitudinal myocardial motion, real-time tissue Doppler imaging (TDI) analysis was performed, and the myocardial tissue velocity profile was obtained from an optimal measuring position set at the basal segment of septum and LV lateral wall from apical four-chamber projections. The mean frame rate was 180 frames per second (FPS) (range 150-210 FPS) for TDI. To reduce the random noise component of the data, we defined 1 mm sample volume. Maximal systolic (S') and early diastolic velocities (E') were measured.

Automated speckle tracking

For 2D STI analysis, tissue harmonic 2D images were scanned at 3 short-axis levels of LV (basal [mitral valve level, MV], midventricular [papillary muscle level, PM], and apical levels [AP]) with an M3S, 5S or 7S probe. The mean frame rate was 50 FPS (range 40-70 FPS). Digital loops were stored on the hard disk of the echocardiography machine, and transferred to a workstation (EchoPAC PC, GE, Horten, Norway) for offline analysis. A line was loosely traced along the LV endocardium at the frame wherein it was best defined. On the basis of this line, the computer automatically created a region of interest (ROI), and the software selected natural acoustic markers moving with the tissue. Automatic frame-by-frame tracking of these markers during the heart cycle (2D STI method) yielded a measure of rotation, V*rot*, strain (S) or strain rate (SR) at any point of myocardium. The LV was divided into 18 segments (6 segments [anteroseptal, anterior, lateral, posterior, inferior, septal]) at 3 levels of LV (MV, PM and AP level) automatically. The software provided an automated tracking score, similar to statistical standard deviation, as feedback of the stability of the regional speckle tracking, ranging from 1.0 to 3.0 in arbitrary units. A tracking score value of ≤ 2.5 was determined as acceptable.

Analysis of left ventricular rotation, rotational rate, and torsion

LV rotation and V*rot* were defined as angular displacement and velocity of angular displacement of LV about its central axis in the short-axis image. They were represented in units of degree (°) and degrees per second (°/sec), respectively. Measuring LV rotation and V*rot* by using STI on the workstation was performed as described previously (10). Clockwise LV rotation as viewed from the apex was expressed as a negative value. Results were subdivided to six segments for regional analysis at each ventricular level, and averaged at each level for analysis of global rotational or torsional motion. Data from at least 3 consecutive beats were averaged for the calculation of LV rotation, V*rot* and torsion. LV torsion was defined as a net-difference of "global LV rotation" between apical and basal short axis planes at each time point (6, 11), and was calculated as the following equation (Fig. 1).

Global torsion (*t*)=Apical global rotation (*t*)-Basal global rotation (*t*)

Peak global torsion was defined as the maximal value of global torsion during the cardiac cycle.

Analysis of left ventricular radial and circumferential strain and strain rate

LV radial motion (motion from the endocardium to the epicardium [12]) and circumferential motion (motion along the curvature of the LV in the parasternal short axis view [12])

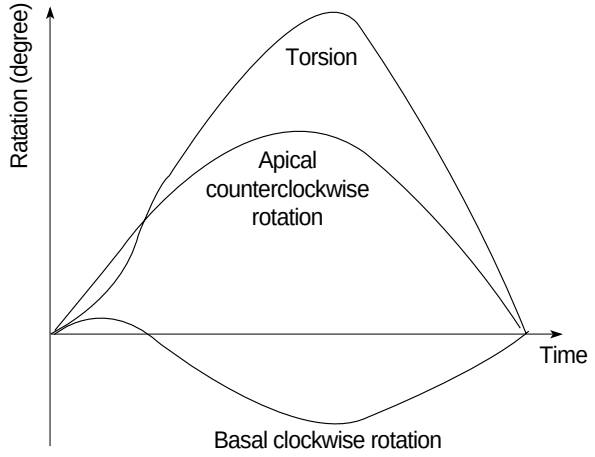

Fig. 1. Measurement of the torsion (degree).
Torsion (*t*)=Apical LV rotation (*t*)-Basal LV rotation (*t*).

were also analyzed as parameters of LV short axis function. LV peak circumferential strain (Sc), systolic strain rate (SRcs), early diastolic strain rate (SRce) and peak radial strain (Sr), systolic strain rate (SRrs), and early diastolic strain rate (SRre) were measured for each segment with the STI method. The SR is equivalent to the spatial gradient of pixel movements. It is characterized by the equation SR=(d[r]-d[r+△r])/△r∗t (d: distance in movement, r: location in space, t: time) (12). The time integral of incremental SR yields S, defined as the fractional change from the original dimension (i.e. the percentage shortening or lengthening of myocardium) (12, 13). %S=(La-Lb)/Lb×100, where La and Lb are the lengths of an infinitesimal material line segment at end diastole and end systole, respectively. Lengthening (or expansion) is positive and shortening (or compression) is negative in this description (13). Data from at least 3 consecutive beats were averaged for the calculation of S and SR. The system calculates mean (global) S and SR values for whole predefined LV segments.

Reproducibility

For intraobserver variability, the observer determined rotation, V*rot*, torsion, Sc, Sr, SRcs, SRce, SRrs, and SRre using the automated program on two images acquired at separate points of time in the same image plane for the same individual. For interobserver comparisons, two independent observers analyzed the same image.

Statistical analysis

To determine whether the differences in the quantitative values between two groups were statistically significant, Student t-test or Chi-square test was performed. Spearman correlation coefficients were obtained to describe first-order relations between torsion (or V*rot*) and several LV functional indices including EF, EDVI, ESVI, velocities of myocardial tissue Doppler, circumferential and radial strain. All of the statistical analyses were performed with Statistica 6.0 software (Statsoft, Tulsa, OK, U.S.A.). All values were presented as mean±standard deviation (SD). A p value less than 0.05 indicated statistical significance for all analyses.

RESULTS

Clinical characteristics of the study population

Global functional parameters measured from conventional transthoracic echocardiogram and long-axis tissue velocities of basal septum and lateral wall are shown in Table 1. DCM patients exhibited significantly increased LVEDVI and ESVI, and decreased EF compared with normal subjects. S' and E' values of LV septum and lateral wall were significantly lower in patients with DCM compared to normal controls.

Image quality and reproducibility of the echocardiographic examination

Image quality was sufficient to allow circumferential and radial S and SR, rotation and V*rot* analysis by the STI method from parasternal short-axis views in 80% of segments (tracking score ≤2.5 as defined by the analysis software). The intraobserver variabilities between measurements of 2 readings were 6.4% for peak rotation, 6.8% for peak systolic V*rot*, and 6.7% for peak early diastolic V*rot*. The interobserver variabilities were found to be 6.4% for peak rotation, 7.1% for peak systolic V*rot*, and 7.3% for peak early diastolic V*rot*. The overall reproducibility of the measurements for rotation and V*rot* by STI method was sufficient.

The intraobserver variabilities between measurements of 2 readings were 5.4% for Sc, 5.8% for Sr, 6.9% for SRcs, 6.7% for SRce, 5.1% for SRrs, and 6.2% for SRre. The interobserver variabilities were found to be 6.7% for Sc, 6.4% for Sr, 7.9% for SRcs, 6.8% for SRce, 7.1% for SRrs, and 6.8% for SRre. The overall reproducibility of the measurements for S and SR by the STI method was sufficient.

Left ventricular rotation, rotational rate, and torsion

In normal controls, apical rotation was consistently counterclockwise (positive) (Fig. 2A), but basal rotation was clockwise (negative) during systole except early systole. Mean values of the peak apical counterclockwise rotation and the peak midventricular and basal clockwise rotation values in normal and DCM children are shown in Table 2. LV rotation was regionally heterogeneous and abnormal in magnitude and patterns in DCM. Apical segmental and global systolic counterclockwise rotation was decreased or abolished (Fig. 2B). Five segmental and global systolic clockwise rotation was

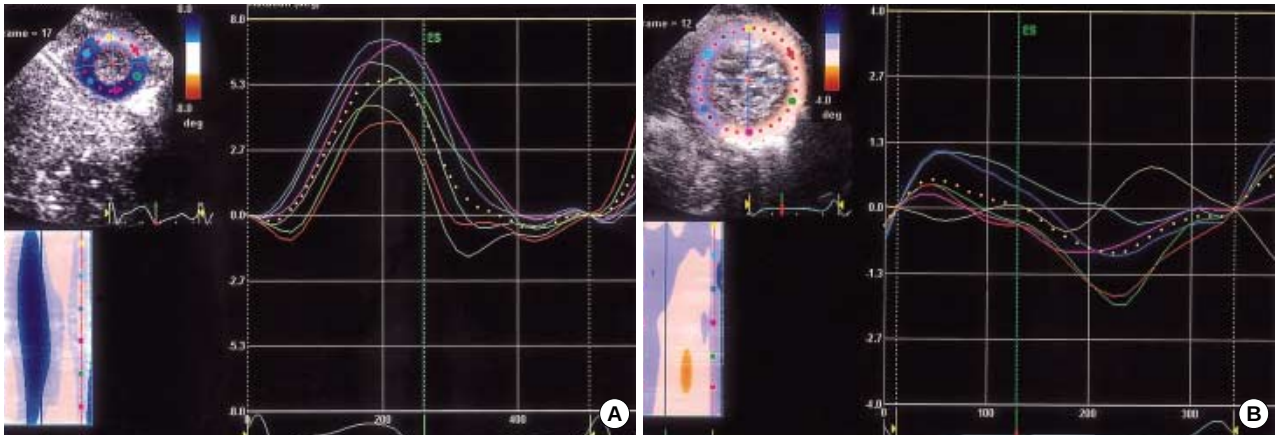

Fig. 2. (A) Profiles of apical segmental and global (dotted line) rotation (°) in a 6 month-old normal boy. Apical rotation was consistently counterclockwise (positive). (B) Profiles of apical segmental and global (dotted line) rotation (°) in a 6 month-old boy with DCM. Apical rotation was clockwise or small counterclockwise, and was markedly heterogenous.

Table 2. Comparison of segmental and global peak rotation (°) at three levels of LV

Peak rotation (°)	Ant sep	Ant	Lat	Post	Inf	Sept	Global
MV normal	-3.6±2.9	-3.0±0.9	-4.0±1.4	-3.1±1.5	-4.9±2.2	-4.8±4.3	-4.2±2.1
MV DCM	-1.5±1.0	-1.4±1.0	-1.9±1.5	-1.2±1.6	-1.9±1.2	-2.5±1.8	-1.8±1.2
p value	0.04	0.004	0.008	0.04	0.002	0.14	0.006
PM normal	-2.6±1.2	-3.9±4.4	-2.8±1.4	-3.4±1.3	-4.9±6.3	-3.6±2.9	-3.9±4.3
PM DCM	-1.7±1.0	-1.7±1.3	-2.1±1.9	-1.6±2.0	-2.1±1.7	-2.0±1.9	-1.8±1.5
p value	0.12	0.16	0.32	0.07	0.2	0.17	0.176
AP normal	7.2±4.0	5±4.0	4.7±4.7	4.7±4.9	6.2±4.2	4.9±4.3	5.9±4.1
AP DCM	-0.1±3.6	-0.02±3.3	-1.2±3.3	-1.7±3.6	-1.4±3.5	-1.1±3.2	-0.9±3.1
p value	0.001	0.01	0.006	0.004	<0.001	<0.001	0.001

Data shown as means±SD.

LV, left ventricular; Ant sep, anteroseptal; Ant, anterior; Lat, lateral; Post, posterior; Inf, inferior; Sept, septal segment; MV normal, measurements at the mitral valve level in normal controls; MV DCM, measurements at the mitral valve level in DCM patients; PM, papillary muscle level; AP, apical level; DCM, dilated cardiomyopathy.

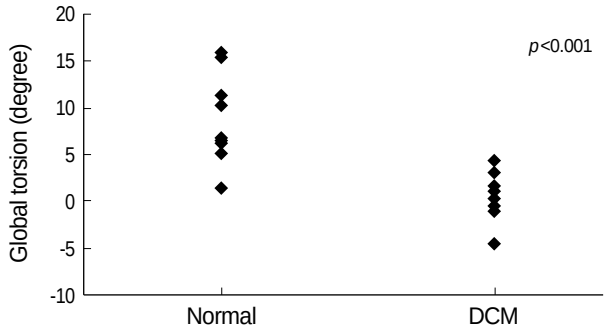

Fig. 3. Comparison of peak global torsion in normal and DCM children. The peak global torsion was significantly decreased in DCM.

decreased significantly at the MV level. One segment at the MV level (septal segment) and six segments at the PM level showed decreased systolic clockwise peak rotation, although they did not reach statistical significance (Table 2). All segmental and global peak torsion was significantly decreased in DCM (peak global torsion; 10.9±4.6° vs. 0.3±2.1°, $p<0.001$) (Fig. 3). Loss of LV torsion occurred mainly by the diminution of counterclockwise apical rotation and was augmented by somewhat less reduction in clockwise basal rotation.

In normal controls, LV apex showed systolic counterclockwise V*rot* and clockwise early diastolic V*rot* (Fig. 4A), and LV base showed systolic clockwise V*rot* and counterclockwise early diastolic V*rot*. In DCM, systolic counterclockwise V*rot* and early diastolic clockwise V*rot* at the apical level were decreased or abolished (apical systolic V*rot*; 43.4±17.6°/sec vs. -7.2±21.4°/sec, $p<0.001$, apical early diastolic V*rot*; -53.4±15.5°/sec vs. 2.9±20.0°/sec, $p<0.001$) (Fig. 4B). Clockwise systolic V*rot* and counterclockwise early diastolic V*rot*, indicating early diastolic recoil, were decreased at the basal level in DCM. The mean values of the peak global systolic and early diastolic V*rot* in normal controls and DCM are listed in Table 3. All DCM patients showed considerable rotational heterogeneity, particularly at the apical level.

In normal controls, approximately 40% to 50% of LV untwisting occurred during isovolumic relaxation (IVR) and 80% to 90% of untwisting was completed by the peak of the early filling velocity (E wave), and the maximum untwist-

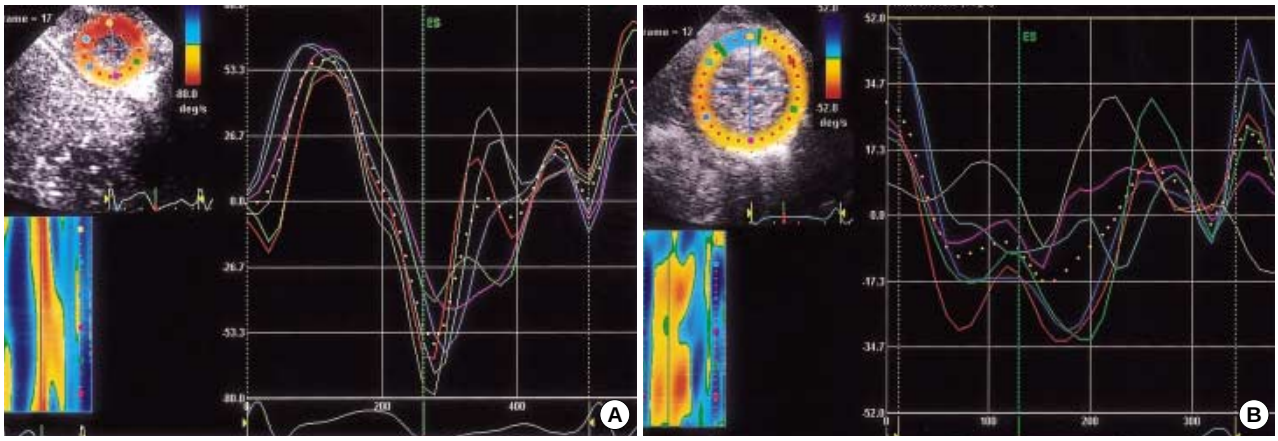

Fig. 4. (A) Profiles of apical segmental and global (dotted line) rotational rate (V*rot*) (°/sec) in a 6 month-old normal boy. LV apex showed systolic counterclockwise (positive) V*rot* and clockwise early diastolic (negative) V*rot*. (B) Profiles of apical segmental and global (dotted line) rotational rate (V*rot*) (°/sec) in a 6 month-old boy with DCM. Systolic counterclockwise V*rot* and early diastolic clockwise V*rot* were abolished. Considerable rotational heterogeneity was noticed particularly at the apical level.

Table 3. Comparison of global peak systolic and early diastolic rotational rate (V*rot*) in normal and DCM patients at three levels of LV

	Global peak systolic V*rot* (°/sec)	Global peak early diastolic V*rot* (°/sec)
MV normal	-35.1±9.7	38.1±19.0
MV DCM	-22.1±13.7	14.8±6.5
p value	0.028	0.002
PM normal	-31.0±8.6	19.6±8.7
PM DCM	-21.7±11.3	11.9±9.1
p value	0.041	0.056
AP normal	43.4±17.6	-53.4±15.5
AP DCM	-7.2±21.4	2.9±20.0
p value	<0.001	<0.001

Data shown as means±SD.
DCM, dilated cardiomyopathy; LV, left ventricular; MV normal, measurements at the mitral valve level in normal controls; MV DCM, measurements at the mitral valve level in DCM patients; PM, papillary muscle level; AP, apical level. V*rot* is given in degrees per second.

ing velocity occurred around the time of mitral valve opening in almost all apical segments of LV. In DCM, the normal counterclockwise apical rotation was not observed, and the apical rotation about the central axis was clockwise or slightly counterclockwise (apical rotation; 5.9±4.1° vs. -0.9±3.1°, $p<0.001$). In DCM patients, in whom the apical rotation was slightly counterclockwise, 30% of LV untwisting occurred during IVR and only 50% to 60% of untwisting was completed by the peak of E wave.

Circumferential and radial strain and strain rate

Circumferential and radial S and SR results are presented in Table 1. In DCM, S, systolic and diastolic SR were markedly regionally heterogeneous along circumferential and radial directions compared to normal controls. Global Sc and Sr in the DCM group were significantly reduced compared to those in normal controls. Global SRcs, SRce, SRrs, and SRre were also significantly reduced.

Table 4. Correlation between global torsion or rotational rate and several left ventricular functional indices in normal and DCM patients

		Correlation coefficient	*p* value
Torsion	EF	0.662	0.002
Torsion	EDVI	-0.594	0.006
Torsion	ESVI	-0.691	0.002
Torsion	MV systolic V*rot*	-0.241	0.299
Torsion	MV early diastolic V*rot*	0.596	0.013
Torsion	AP systolic V*rot*	0.874	<0.001
Torsion	AP early diastolic V*rot*	-0.755	<0.001
Torsion	Septal S'	0.639	0.002
Torsion	Septal E'	0.724	<0.001
Torsion	Lateral S'	0.360	0.119
Torsion	Lateral E'	0.565	0.009
Torsion	Radial strain	0.714	0.009
Torsion	Circumferential strain	-0.893	0.004
MV systolic V*rot*	Septal S'	-0.545	0.021
MV early diastolic V*rot*	Septal E'	0.588	0.005
AP systolic V*rot*	Septal S'	0.537	0.013
AP early diastolic V*rot*	Septal E'	-0.681	0.003

DCM, dilated cardiomyopathy; EF, ejection fraction; EDVI, end diastolic volume index; ESVI, end systolic volume index; MV systolic V*rot*, peak systolic rotation rate at the mitral valve level; AP, at the apical level; S', peak systolic velocity of myocardial tissue Doppler at LV base; E', peak early diastolic velocity of myocardial tissue Doppler at LV base.

Correlation between torsion and other functional indices

Table 4 shows the relations between torsion and other functional indices of LV. Global torsion inversely correlated with LVEDVI (r=-0.594, $p=0.006$) and ESVI (r=-0.691, $p=0.002$).

Torsion correlated positively with EF (r=-0.662, p=0.002). Torsion closely correlated with systolic and early diastolic V*rot* of LV apex. There were close relations between torsion and the indices of longitudinal function, i.e. septal S' and E'. Torsion correlated more closely with septal E' than S'. Tight positive relations were also found between torsion and LV short-axis functional indices, i.e. LV radial and circumferential strain. Systolic and early diastolic V*rot* of apex and base correlated closely with basal septal S' and E', respectively (Table 4).

DISCUSSION

A recent study reported assessment of LV torsion with the TDI method (11). However, such method has limitations of using only 2 sampling points for rotational calculation, and cannot assess the regional LV rotational behavior. From a single conventional gray scale data set, the 2D STI method allows exploration of complex features of heart motion inaccessible to current echocardiographic techniques, and it is also possible to quantify regional rotation and V*rot* in the short-axis view of a beating heart (7). The STI estimation of LV torsion was concordant with those analyzed by tagged MRI and also showed good agreement with those by TDI (10).

The present study revealed that apical rotation was consistently counterclockwise from infancy to adolescence. It is consistent with the result of the previous study that underwent assessment of LV torsion and untwisting rate by TDI (4). However, the result of the present study for basal rotation was different from the previous study. This difference might be due to the different methodologies of two studies. From infancy to adolescence, basal rotation was clockwise during systole except a short period of early systole. The initial small counterclockwise basal twist should be related to the fact that the subendocardium is electrically activated earlier during systole, and the subsequent activation and contraction of the basal subepicardial fibers causes a counter-rotating torque and clockwise twist throughout the remainder of systole (14). Several studies have reported that the directions of myocardial fibers varied gradually from subendocardium to subepicardium, and the subendocardium is composed of myocardial fibers oriented in different directions from those of the subepicardium (14-17).

DCM is associated with LV remodeling including dilatation, wall thinning, and reduction in fiber angles. Tachycardia-induced dilated cardiomyopathic hearts showed marked alterations in diastolic LV torsional dynamics (5). The measurements of LV tosion with MRI demonstrated impaired torsion in DCM patients and persistent abnormal torsion after partial left ventriculectomy (6). Our data revealed that LV torsion mechanics were markedly changed throughout the cardiac cycle in DCM. The maximal torsion was not only reduced, but it was also delayed and disorganized. This is consistent with the previous studies (5, 18). Loss of LV torsion occurred mainly by the diminution of counterclockwise apical rotation and was augmented by somewhat less reduction in clockwise basal rotation. In normal controls, approximately 40% to 50% of LV untwisting occurred during IVR and 80% to 90% of untwisting was completed by the peak of the early filling velocity (E wave), which is consistent with the previous report (19). It was reported that peak untwisting preceded peak IVPG, which in turn preceded peak early filling (19). It is known that LV untwisting contributes to the large rapid pressure fall of IVR and the additional pressure fall after mitral valve opening to peak early filling of LV. In DCM, the sufficient counterclockwise apical rotation was not observed, and the apical rotation about the central axis was clockwise or slightly counterclockwise. In DCM patients, in whom the apical rotation was slightly counterclockwise, 30% of LV untwisting occurred during IVR, and only 50% to 60% of untwisting was completed by the peak of E wave. The impairment of untwisting should have caused the reduction of intraventricular pressure gradient and the impairment of diastolic filling in DCM.

All DCM patients showed considerable rotational heterogeneity, particularly at the apical level. The marked heterogeneity of regional LV function has frequently been noted in patients with non-ischemic DCM (18, 20-22). Nonhomogeneous twisting and untwisting may in itself have detrimental effects on ventricular performance, since mechanical work is wasted when some regions are in process of twisting or untwisting while the other regions are not. Possible mechanisms for functional heterogeneity include regional variations in wall stress, myocardial contractile efficiency, oxidative metabolism, myocardial perfusion, and interstitial fibrosis (18, 20, 22, 23). With depressed, delayed and disorganized untwisting, reflecting ineffective uncoiling of the myocardium, the DCM ventricle fails to generate the effective pressure fall of IVR and the subsequent suction phase.

The mechanisms underlying the changes in torsion dynamics are unknown but probably encompass many factors associated with cardiomyopathic conditions, including LV dilatation, remodeling of the cardiomyocytes and connective tissue matrix, slowed transmural fiber activation, and alterations in excitation-contraction coupling (24-30).

The impaired torsion was associated with global ventricular dysfunction. Global torsion correlated inversely with LVEDVI and ESVI, and correlated positively with EF. Torsion and V*rot* also correlated positively with the indices of LV long axis function, i.e., S' and E' of myocardial tissue Doppler of LV base. Torsion correlated closely with apical early diastolic V*rot* and E', and suggests that the impairment of torsion is related to the impairment of early diastolic LV untwisting and lengthening. In addition to these relations, there was a close correlation between torsion and LV short-axis function. Torsion closely correlated with circumferential and radial strain of LV base. It is interesting that torsion is related to all three components of LV function, and these three com-

ponents are altered in the same way as torsion.

Ventricular myocardium is now considered as a continuous structure, in which myofibers are organized into laminar sheets about four-cell thickness and the orientation of the sheet varies smoothly through the ventricular walls, and there are some branches between adjacent layers (15, 16). The smoothly changing muscle fiber directions and anastomoses between layers partly explain the relations between torsion and other components of LV function. According to the concept of ventricular myocardial band, septum contains a right angle cross-striation of oblique longitudinal fibers that are directed toward and away from the conical apical tip (1). The oblique orientation of muscle fibers of the LV free wall and septum allows the twisting required in ejecting blood into high systemic vascular resistance. As ventricle dilates, the oblique fiber orientation changes to more transverse direction, and this may cause the reduction of twisting, thickening, and longitudinal shortening of LV in DCM. Contraction of the other oblique fibers which cross over the previous oblique fibers gives rise to lengthening and untwisting of the entire ventricular mass (31). Loss of obliquity of ascending segment may cause the reduction of untwisting and longitudinal lengthening for suction filling.

Contemporary experimental and clinical investigations unequivocally support the attitude that only powerful suction force, developed by the normal ventricles, could be able to produce an efficient filling of the ventricular cavities (32-34). According to the ventricular myocardial band concept, this force uses the systolic mechanism (i.e. contraction) for ventricular filling during the diastole. However, the mechanisms responsible for ventricular filling are very difficult to understand and explain even with the present concept of ventricular myocardial band, and still there are a lot of points to be clarified.

LV torsion is a critical aspect of cardiac biomechanics and important for normal ejection and suction (31). In DCM ventricles, regionally heterogeneous, decreased and delayed systolic torsion and loss of early diastolic recoil contribute to LV systolic and diastolic dysfunction. Impairment of torsion correlates closely with LV longitudinal, radial, and circumferential contraction. Assessment of LV rotation with the STI provides not only peak rotation and torsion but also the profile curve (the rotational velocity over time), may facilitate the serial evaluations of the LV torsional behavior in clinical settings and give new biomechanical concepts for better management of patients with DCM.

Several limitations should be noted in this study. First, the success of measurements of rotation, V*rot*, S or SR by the STI method was dependent on the quality of 2D echocardiographic images. STI-based methods do not track well in walls with poor B-mode data, in which the unique speckle pattern of each point defining the segments in the myocardium cannot be repeated perfectly from frame to frame. Second, although there was no significant difference in age distribution between the two study groups, normal values of peak rotation, torsion, and V*rot* of each age group measured with STI were not presented in this study. The study populations of patients and controls were small in size, and aging factors were not considered in this study. Third, global torsion was used to evaluate the correlation between torsion and the other indices of global function; however, there was marked heterogeneity of regional wall motion in DCM and this heterogeneity was not considered in this approximation. Lastly, factors such as medical therapy, which could potentially affect torsion and untwisting, were not considered in this study.

REFERENCES

1. Buckberg GD, Clemente C, Cox JL, Coghlan HC, Castella M, Torrent-Guasp F, Gharib M. *The structure and function of the helical heart and its buttress wrapping. IV. Concepts of dynamic function from the normal macroscopic helical structure. Semin Thorac Cardiovasc Surg 2001; 13: 342-57.*
2. Burleson KO, Schwartz GE. *Cardiac torsion and electromagnetic fields: the cardiac bioinformation hypothesis. Medical Hypotheses 2005; 64: 1109-16.*
3. Yun KL, Niczyporuk MA, Daughters GT, Ingels NB Jr, Stinson EB, Alderman EL, Hansen DE, Miller DC. *Alterations in left ventricular diastolic twist mechanics during acute human cardiac allograft rejection. Circulation 1991; 83: 962-73.*
4. Notomi Y, Srinath G, Shiota T, Martin-Miklovic MG, Beachler L, Howell K, Oryszak SJ, Deserranno DG, Freed AD, Greenberg NL, Younoszai A, Thomas JD. *Maturational and adaptive modulation of left ventricular torsional biomechanics: Doppler tissue imaging observation from infancy to adulthood. Circulation 2006; 113: 2534-41.*
5. Tibayan FA, Lai DT, Timek TA, Dagum P, Liang D, Daughters GT, Ingels NB, Miller DC. *Alterations in left ventricular torsion in tachycardia-induced dilated cardiomyopathy. J Thorac Cardiovasc Surg 2002; 124: 43-9.*
6. Setser RM, Kasper JM, Lieber ML, Starling RC, McCarthy PM, White RD. *Persistent abnormal left ventricular systolic torsion in dilated cardiomyopathy after partial left ventriculectomy. J Thorac Cardiovasc Surg 2003; 126: 48-55.*
7. Suhling M, Jansen C, Arigovindan M, Buser P, Marsch S, Unser M, Hunziker P. *Multiscale motion mapping; a novel computer vision technique for quantitative, objective echocardiographic motion measurement independent of Doppler; first clinical description and validation. Circulation 2004; 110: 3093-9.*
8. Helak JW, Reichek N. *Quantification of human left ventricular mass and volume by 2-dimensional echocardiography: in vivo anatomic validation. Circulation 1981; 63: 1398-407.*
9. Sutton M, Plappert T, Spigel A, Raichlen J, Douglas P, Reichek N, Edmunds L. *Early prospective changes in left ventricular chamber size, architecture, and function in aortic stenosis and aortic regurgitation and their relation to intraoperative changes in afterload: a prospective 2-dimensional echocardiographic study. Circulation 1987; 76: 77-89.*

10. Notomi Y, Lysyansky P, Setser RM, Shiota T, Popovic JB, Martin-Miklovic MG, Weaver JA, Oryszak SJ, Greenberg NL, White RD, Thomas JD. *Measurement of ventricular torsion by two-dimensional ultrasound speckle tracking imaging. J Am Coll Cardiol 2005; 45: 2034-41.*
11. Notomi Y, Setser RM, Shiota T, Martin-Miklovic MG, Weaver JA, Popovic JB, Yamada H, Greenberg NL, White RD, Thomas JD. *Assessment of left ventricular torsional deformation by Doppler tissue imaging: validation study with tagged magnetic resonance imaging. Circulation 2005; 111: 1141-7.*
12. Becker M, Bilke E, Kühl H, Katoh M, Kramann R, Franke A, Bucker A, Hanrath P, Hoffmann R. *Analysis of myocardial deformation based on pixel tracking in 2D echocardio-graphic images allows quantitative assessment of regional left ventricular function. Heart 2006; 92: 1102-8.*
13. Toyoda T, Bada H, Akasaka T, Akiyama M, Neishi Y, Tomita J, Sukmawan R, Koyama Y, Watanabe N, Tamano S, Shinomura R, Komuro I, Yoshida K. *Assessment of regional myocardial strain by a novel automated tracking system from digital image files. J Am Soc Echocardiogr 2004; 17: 1234-8.*
14. Yun KL, Miller DC. *Torsional deformation of the left ventricle. J Heart Valve Dis 1995; 4: 214-22.*
15. LeGrice IJ, Smail BH, Chai LZ, Edgar SG, Gavin JB, Hunter PJ. *Laminar structure of the heart: ventricular myocyte arrangement and connective tissue architecture in the dog. Am J Physiol 1995; 269: 571-82.*
16. Arts T, Costa KD, Covell JW, McCulloch AD. *Relating myocardial laminar structure to shear strain and muscle fiber orientation. Am J Physiol Circ Physiol 2001; 280: 2222-9.*
17. Spotnitz HM. *Macro design, structure, and mechanics of the left ventricle. J Thorac Cardiovasc Surg 2000; 119: 1053-77.*
18. Young AA, Dokos S, Powell KA, Sturm B, McCulloch AD, Starling RC, McCarthy PM, White RD. *Regional heterogeneity of function in nonischemic dilated cardiomyopathy. Cardiovasc Res 2001; 49: 308-18.*
19. Notomi Y, Martin-Miklovic MG, Oryszak SJ, Shiota T, Deserranno D, Popovic ZB, Garcia MJ, Greenberg NL, Thomas JD. *Enhanced ventricular untwisting during exercise: a mechanistic manifestation of elastic recoil described by Doppler tissue imaging. Circulation 2006; 113: 2524-33.*
20. Bach DS, Beanlands RS, Schwaiger M, Armstrong WF. *Heterogeneity of ventricular function and myocardial oxidative metabolism in nonischemic dilated cardiomyopathy. J Am Coll Cardiol 1995; 25: 1258-62.*
21. Hayashida W, Kumada T, Nohara R, Tanio H, Kambayashi M, Ishikawa N, Nakamura Y, Himura Y, Kawai C. *Left ventricular regional wall stress in dilated cardiomyopathy. Circulation 1990; 82: 2075-83.*
22. Juillière Y, Marie PY, Danchin N, Gillet C, Paille F, Karcher G, Bertrand A, Cherrier F. *Radionuclide assessment of regional differences in left ventricular wall motion and myocardial perfusion in idiopathic dilated cardiomyopathy. Eur Heart J 1993; 14: 1163-9.*
23. Nakayama Y, Shimizu G, Hirota Y, SaitoT, Kino M, Kitaura Y, Kawamura K. *Functional and histopathologic correlation in patients with dilated cardiomyopathy: an integrated evaluation by multicariate analysis. J Am Coll Cardiol 1987; 10: 186-92.*
24. Chow E, Woodard JC, Farrar DJ. *Rapid ventricular pacing in pigs: an experimental model of congestive heart failure. Am J Physiol 1990; 258: 1603-5.*
25. Spinale FG, Zellner JL, Johnson WS, Eble DM, Munyer PD. *Cellular and extracellular remodeling with the development and recovery from tachycardia-induced cardiomyopathy: changes in fibrillar collagen, myocyte adhesion capacity and proteoglycans. J Mol Cell Cardiol 1996; 28: 1591-608.*
26. Spinale FG, Tomita M, Zellner JL, Cook JC, Crawford FA, Zile MR. *Collagen remodeling and changes in LV funcition during development and recovery from supraventricular tachycardia. Am J Physiol 1991; 261: 308-18.*
27. Spinale FG, Coker ML, Thomas CV, Walker JD, Mukherjee R, Hebbar L. *Time-dependent changes in matrix metalloproteinase activity and expression during the progression of congestive heart failure: relation to ventricular and myocyte function. Circ Res 1998; 82: 482-95.*
28. Delhaas T, Arts T, Prinzen FW, Reneman RS. *Regional electrical activation and mechanical function in the partially ischemic left ventricle of dogs. Am J Physiol 1996; 271: 2411-20.*
29. O'Rourke B, Kass DA, Tomaselli GF, Kaab S, Tunin R, Marban E. *Mechanisms of altered excitation-contraction coupling in canine tachycardia-induced heart failure, I: experimental studies. Circ Res 1999; 84: 562-70.*
30. Winslow RL, Rice J, Jafri S, Marban E, O'Rourke B. *Mechanisms of altered excitation-contraction coupling in canine tachycardia-induced heart failure, II: model studies. Circ Res 1999; 84: 571-86.*
31. Torrent-Guasp F, Kocica MJ, Corno AF, Komeda M, Cox J, Flotats A, Ballester-Rodes M, Carreras-Costa F. *Systolic ventricular filling. Eur J Cardiothorac Surg 2004; 25: 376-86.*
32. Yip G, Wang M, Zhang Y, Fung JW, Ho PY, Sanderson JE. *Left ventricular long axis function in diastolic heart failure is reduced in both diastole and systole: time for redefinition? Heart 2002; 87: 121-5.*
33. Henein MJ, Gibson DG. *Normal long-axis function. Heart 1999; 81: 111-3.*
34. Henein MJ, Gibson DG. *Long-axis function in disease. Heart 1999; 81: 229-31.*